PCCP

Accepted Manuscript

ROYAL SOCIETY OF CHEMISTRY

www.rsc.org/pccp

Propagation of the change in the membrane potential using the biocell-model

Yoshinari Takano, Osamu Shirai†, Yuki Kitazumi and Kenji Kano

Division of Applied Life Sciences, Graduate School of Agriculture, Kyoto University, Sakyo, Kyoto 606-8502, Japan

† To whom correspondence should be addressed.

E-mail: shiraio@kais.kyoto-u.ac.jp

Abstract

A new model system, which has two sites (the potential-sending and the potential-receiving sites), on the nerve conduction was constructed by use of some liquid-membrane cells which mimic the function of the K^+ and Na^+ channels. The model system setup was such that the membrane potential of the K^+-channel cell (resting potential) is different from that of the Na^+-channel cell (action potential). Initially, the K^+-channel cell in the potential-sending site was connected to that in the potential-receiving site. After the switch from the K^+-channel cell to the Na^+-channel cell at the potential-sending site, the membrane potential of the K^+-channel cell at the potential-receiving site began to vary with the generation of the circulating current. By placing several K^+-channel cells in parallel at the potential-receiving site, the propagation mechanism on the action potential was interpreted and the influence of the resistor and the capacitor on the propagation was evaluated.

Keywords: Liquid membrane, membrane potential, ion transport, propagation, circulating current, ion channel

1. Introduction

In nerve cells, the change in the membrane potential is mainly propagated by the function of the K^+ and Na^+ channels.[1-6] The membrane potential of the nerve cells is usually determined by the ratio of the concentration of K^+ of the inside to that of the outside the cell. It is called the resting potential. When neurotransmitters combine with channel-type receptors at the synapse, Na^+ is mainly transported from the outside to the inside of the cell. The membrane potential is changed from the resting potential to the action potential determined by the ratio of the concentration of Na^+ on the inside to that on the outside the cell. The change in the membrane potential is propagated along the axon to the axon terminal. As the voltage-gated Na^+ channels, which have short open-lives (about 1 ms), are opening successively in the axon, the membrane potential in the axon is changed to the action potential toward the axon terminal. Thus, the propagation of the change in the membrane potential is directionally conducted along the axon toward the synaptic terminus.

In physiological experiments, the directional propagation of the action potential has been usually recorded by the voltage-clamp method.[7] Since the local currents at several parts of the axon surfaces are measured under the constant membrane potential, the local currents are converted to the potential differences by considering the change in the permeability.[7] Thus, the membrane potential cannot be directly recorded by this method. In addition, the expression mechanism of the overshoot which appears before the membrane potential goes back to the rest potential cannot be resolved.

The author's group has proposed a new mechanism for the propagation of the change in the membrane potential using a U-shaped organic-liquid-membrane cell system.[8-9] The cell has two liquid membranes which were placed between two aqueous

phases. In this case, the interfacial potentials were regulated by the transfer of two ion species of which the standard potentials for the ion transfer across the interface between the aqueous and 1,2-dichloroethane (DCE) are different from each other. We confirmed that the change in the membrane potential was propagated by the generation of the circulating current through two liquid membrane sites (the potential-sending and the potential-receiving sites), and that the magnitude of the circulating current determined the threshold to cause the change in the membrane potential by considering the electroneutrality and the mass-balance.[8-11] In addition, it has been found that the *iR* drop generated by the resistor in the electric circuit depresses and slows down the propagation of the change in the membrane potential and that the charging current generated by the capacitor in the electric circuit delays the propagation, analogous to the nerve transmission.[10]

In the present study, a new model system of the nerve conduction was constructed by use of some liquid-membrane cells that mimic the function of the K^+ and Na^+ channels. The membrane potential of the liquid-membrane cell, which mimics the function of the K^+ channel (K^+-channel cell), is considered to be the resting potential. On the other hand, that which mimics the function of the Na^+ channel (Na^+-channel cell) is considered to be the action potential. The membrane potential at the potential-receiving site was changed with the generation of the circulating current by switching from the K^+-channel cell to the Na^+-channel cell at the potential-sending site. The propagation mechanism of the action potential is discussed based on the change in the interfacial potentials of all the cells and on the generation of the local circulating current based on the electroneutrality.

Experimental

Reagents and Chemicals

Sodium tetrakis[3,5-bis(trifluoromethy)phenyl]borate (NaTFPB) was prepared in a similar manner as previously reported.[12] The $TFPB^-$ salt of tetrabutylammonium (TBA^+) was obtained by mixing a DCE solution of NaTFPB with that of TBACl (Tokyo Kasei Chemical Co.). DCE and nitrobenzene (NB) were purchased from the Wako Pure Chemical Co. All the other chemicals were of analytical reagent grade and were used without further purification. The PTFE membrane filter T100A025A (pore size: 1 μm, thickness: 75 μm) was obtained from Advantec, and was used in order to stabilize the liquid-liquid interface.

Apparatus

Potentiometric measurements were performed on a potentiostat/galvanostat, model HA-1010mM4A (Hokuto Denko Co.), and several HE-106A electrometers (Hokuto Denko Co.). The circulating current was measured by several HM-103 (Hokuto Denko Co.) and HM-103A (Hokuto Denko Co.) ammeters. Each data was recorded by use of an A/D converter, model GL900 (Graphtec Co.). The cell system was made to mimic the nerve conduction between two nodes of Ranvier in the axon (Fig. 1A). An MR-4-3Z (FUJISOKU) rotary switch was placed within the electric circuit of the cell system, as shown in Fig. 1B.

Electrochemical Measurements

The electrochemical cell system combined with five liquid-membrane cells, which were composed of two aqueous phases (W1 and W2) and a nitrobenzene phase (NB), was prepared as

illustrated in Figs. 1B and 1C. The cell system was divided in two part; the potential-sending site and the potential-receiving site in order to mimic the nerve conduction such that the change in the membrane potential is propagated from one site to another site along the axon. The liquid membrane cell, which showed the rest potential (RP cell), and the liquid membrane cell, which showed the action potential (AP cell), were placed on the potential-sending site. The cell configurations of the RP and AP cells were described by Eqs. (1) and (2). At the potential-receiving site, three liquid membrane cells, which indicated the rest potential (Rec cell), were constructed. The cell configuration of the Rec cell is described by Eq. (3).

W1	M	W2	
1×10^{-3} M KCl	1×10^{-3} M KTFPB	2×10^{-2} M KCl	(1)
9.5×10^{-3} M $MgCl_2$	1×10^{-2} M TBATFPB		
(RE1)		(RE2)	

W1	M	W2	
2×10^{-2} M NaCl	4×10^{-3} M NaTFPB	1×10^{-3} M NaCl	(2)
	1×10^{-2} M TBATFPB	9.5×10^{-3} M $MgCl_2$	
	2×10^{-2} M DB18C6		
(RE3)		(RE4)	

W1	M	W2	
1×10^{-3} M KCl	1×10^{-4} M KTFPB	2×10^{-2} M KCl	(3)
9.5×10^{-3} M $MgCl_2$	1×10^{-2} M TBATFPB		
(RE5)		(RE6~8)	

Here, DB18C6 is dibenzo-18-crown-6 and was used to stabilize Na^+ in NB and to facilitate the transfer of Na^+ at the interface between the aqueous and NB. TBATFPB was added as a supporting electrolyte in M to lower the solution resistance. Ag|AgCl electrodes were immersed in W1 and W2 of each cell in order to measure the potential. All the W1 and W2 phases of the

five cells contained 2×10^{-2} M Cl^- and were electrically connected to each other. The membrane area of the RP and the AP cells were 3.5 cm^2 and those of the Rec cells were 1.3 cm^2. In the electric circuit of the potential-receiving site, resistors mimic the solution resistances between the potential-sending site and the potential-receiving site and capacitors evoke the charging currents generated at the surface of cell membranes.

Results and Discussion

Propagation of the Change in the Membrane Potential and Effect of Distance in Axon

When the connection of the Rec cells was switched from the RP cell to the AP cell, the change in the membrane potential was caused with the circulating current in each cell. Since each phase contains sufficient electrolyte, the membrane potential of each cell (E_{W2-W1}) is determined by Eq. (4).

$$E_{W2-W1} = E_{W2|M} - E_{W1|M} \quad (4)$$

where $E_{W1|M}$ and $E_{W2|M}$ denote the potential difference at the W1|M and W2|M interfaces, respectively.

Fig. 2(A) shows the change in the membrane potentials of the AP and the Rec cells with the resistor (R = 10 kΩ). Initially, the membrane potential of each cell (E_{W2-W1}) at the potential-receiving site (Rec cells 1-3) showed the resting potential. The E_{W2-W1} values of Rec cells 1-3 were −75.8, −71.6 and −69.1 mV, respectively. Although the ionic compositions of Rec cells 1-3 were equivalent, the membrane potentials of Rec cells 1-3 were slightly different from each other. It seems to be mainly caused by variations in the potentials of the reference electrodes and the area of each interface. On the other hand, the E_{W2-W1} values of the RP and the AP cells on open circuit were −73.2 and +75.8 mV, respectively. Fig. 2(B) shows the change in

the current that flowed through each cell at the same time. When the Rec cells were connected to the RP cell (t = –20 s), the membrane potentials were not changed and no current was observed. When the Rec cells were connected to the RP cell, the W1|M and W2|M interfaces were depolarized by the distribution of K^+. Accordingly, all the interfacial potentials ($E_{W1|M}$ and $E_{W2|M}$ of every cell) were determined by the ratio of the K^+ concentration in W1 and W2 to that in M. Subsequently, the membrane potentials of all the cells were changed and the circulating currents were generated through the AP and the Rec cells when the Rec cells were connected to the AP cell by switching (t = 0 s). The lower resistance between the AP cell and the Rec cell had the higher change in the membrane potential and a higher current was generated. The change in the membrane potential of Rec cell 1, of which the resistance between the AP cell and the Rec cell was lower than the other Rec cells, was the highest, and the current that flowed through the Rec1 cell the highest. Thus, the circulating current generated by switching from the RP cell to the AP cell produced the change in the interfacial potentials, and the membrane potentials changed at the same time. The membrane potentials of the Rec1-3 cells became almost constant values at t = 80 s and were +47.7, +4.7 and –5.6 mV, respectively. In addition, the time courses of the difference between the membrane potential of the Rec cells 1-3 were expressed by followed Eqs.(5) and (6).

$$E_{\mathrm{W2-W1,Rec1}} - E_{\mathrm{W2-W1,Rec2}} = \left(i_{\mathrm{Rec2}} + i_{\mathrm{Rec3}}\right)R \quad (5)$$

$$E_{\mathrm{W2-W1,Rec2}} - E_{\mathrm{W2-W1,Rec3}} = i_{\mathrm{Rec3}}R \quad (6)$$

where $E_{\mathrm{W2-W1,\ Rec1\text{-}3}}$ represents the membrane potential of the Rec1-3 cells and $i_{\mathrm{Rec1\text{-}3}}$ indicates the current that flowed through the Rec1-3 cells. Finally, when the connection of the Rec cells 1-3 was replaced from the AP cell to the RP cell, the opposite currents were generated through all the cells, and the membrane potentials went back to the resting potentials. Although the hyperpolarization has been frequently reported during nerve conduction,[6,7] the hyperpolarization did not appear in the present case. On the other hand, the circulating current that flowed in the

opposite direction was observed. In general, assuming that the conductances of the Na^+ channel, the K^+ channel and lipid bilayers are constant, the change in the current can be converted to the change in the membrane potential according to Ohm's law during nerve conduction.[7] Thus, the transformation makes the membrane potential more negative than the resting potential. Under the condition, however, K^+ is pumped from W1 to W2 as opposed to the concentration gradient, as shown in Fig. S1.

Fig. 3 illustrates the imaginary steady-state voltammograms for the ion transfer of K^+ and Na^+ by considering the transfer potentials of K^+ and Na^+ from W to NB (242 and 354 mV *vs*. TPhE, respectively) and their concentrations.[13] Taking into account the constant of the complex formation of DB18C6 with Na^+ and their concentrations in M, the apparent standard potential for the transfer of Na^+ is estimated to be 23 mV *vs*. TPhE. A dotted line or a dashed line shows the ion transfer current due to the transfer of Na^+ from W to M or from M to W. Since whole cells were connected in parallel, the total current between W1 and W2 was always zero. When the Rec cells 1-3 were connected with the RP cell (t = –20 s), the membrane potentials of the Rec cells 1-3 were almost equivalent to each other and the current did not flow at each cell. After the connection of the Rec cells with the AP cell (t = 0 s), the circulating current flowed by ion transfer through each cell in order to maintain the electroneutrality in every phase. The membrane potential and the interfacial potentials of each cell then mutually changed. While the interfacial potential changes to maintain the sum of the currents observed at the W1|M interfaces to zero, K^+ was transported from M to W1 in Rec cells 1-3 and Na^+ was transported from W1 to M in the AP cell. Similarly, K^+ was transported from W2 to M in Rec cells 1-3, and Na^+ was transported from M to W2 in the AP cell when the interfacial potential was changed. In each cell, the magnitude of the current that flows at the W2|M interface is equivalent to that which flows at the W1|M interface. Since the potential of M is regarded as a standard on the imaginary steady-state voltammogram, the current that flows at the W2|M interface is opposite

to that at the W1|M interface. Thus, the circulating current was generated between the Rec cells 1-3 and the AP cell while the interfacial potential mutually varied. By considering these facts, the closed circle (●) on the solid line of the imaginary steady-state voltammogram shows the interfacial potential of each cell after the switch from the RP cell to the AP cell. In addition, the limiting currents (i_1, i_2 and i_3) were determined by the transport of K^+ from M to W1 in Rec cells 1-3, and the summation of the current that flowed in Rec cells 1-3 was equivalent to the current that flowed in the AP cell.

Effect of Resistors in the Electric Circuit on the Propagation of the Change in the Membrane Potential

Fig. 4 represents the time courses of E_{W2-W1} (a) and the current (b) in each Rec cell with different resistors (R = 5, 10, 20 and 51 kΩ) connected within the electric circuits as shown in Fig. 1. The change in the membrane potential of the Rec1 cell was minor and slightly increased with an increase in the magnitude of the resistor of the Rec2 and Rec3 cells. On the other hand, the changes in the membrane potential of the Rec2 and Rec3 cells decreased with an increase in the resistance. The E_{W2-W1} values of the Rec2 cell were −14, −25, −39 and −54 mV at t = 5 s (R = 5, 10, 20 and 51 kΩ, respectively). Similarly, E_{W2-W1} of the Rec3 cell were −24, −40, −55 and −66 mV, respectively, at t = 5 s. The current that flowed through the Rec1 cell slightly increased with an increase in the resistance. The currents that flowed through the Rec2 cell using different resistors (R = 5, 10, 20 and 51 kΩ) were 4.6, 3.5, 2.6 and 1.6 μA, respectively. The currents of the Rec3 cell (R = 5, 10, 20 and 51 kΩ) at t = 5 s were then 3.7, 2.4, 1.3 and 0.5 μA, respectively. By considering the imaginary steady-state voltammogram as indicated in Fig. 3, the magnitude of the circulating current of each cell is determined by the transport of K^+ at the W1|M interface.

It is clear that the circulating current decreased by the effect of the *iR* drop generated by the insertion of the resistor. That is the reason why the change in the membrane potential decreased.

In fact, the width of an axon is so narrow (0.2~2 μm in diameter) and the length of the axon ranged from several millimeter to about 1 m.[4] Accordingly, the change in the membrane potential is affected by the significant influence of the *iR* drop caused by the solution resistance. If the current generated by the ion transport of the ligand-gated Na^+ channels at the synapse (like the current generated by the ion transfer at the potential-sending site in this work) is not sufficient, the change in the membrane potential hardly propagated to the terminal of the axon.[14]

Effect of Capacitor in the Circuit on the Propagation of the Membrane Potential

Fig. 5 indicates the time courses of E_{W2-W1} (a) and the current (b) in each Rec cell with different capacitors (C = 10, 50 and 100 μF) connected within the electric circuit. Just after the connection with the AP cell (t = 0 s), E_{W2-W1} was changed in each Rec cell. The effect of the charging current was scarcely observed in the Rec1 cell. On the other hand, the change in the membrane potential was delayed at the Rec2 or Rec3 cell. Similarly, the rate of the increasing current just after the switching decreased with an increase in the capacitance. Initially, each capacitor was charged as the membrane potential was changed by switching from the RP cell to the AP cell. Secondly, the current due to the ion transfer was generated. Thus, this means that the current needed for the change in the membrane potential decreases by charging the capacitors. The charging current delayed the change in both the membrane potential and the generation of the current through the Rec cells. In addition, the value of each cell at t = 5 s was almost equivalent to that observed at t = 5 s in the absence of any capacitor.

In this work, the change in the membrane potential is delayed by charging to capacitor. Actually, it is well-known that the propagation of the change in the membrane potential is

delayed by the charging at the interfaces of the lipid bilayers of nerve cells.[15,16] The role of the voltage-gated Na^+ channels, which have a short opening-life (about 1 ms), is important. It is considered that the delay of the potential propagation produces serious problems in neurotransmission. In unmyelinated axons, since the membrane is bare and has high capacitance, the width of the axon is broad and the current due to the ion transfer is high in order to reduce the influence of the charging current.[17,18] On the other hand, as for higher animals, the area of the bare lipid bilayers of the axon surface is extremely small due to the development of the myelin sheath.[4,6,16] Therefore, the capacitance of the cell membrane can be reduced, and does not repress the propagation of the membrane potential although the current generated by the ion transfer across the lipid bilayers is low as the axon is narrow.

Conclusions

In the present work, a new model system related to nerve conduction was developed using some liquid-membrane cells that mimic the function of the K^+ and Na^+ channels. The propagation of the change in the membrane potential successfully occurred by switching the cell of the potential-sending site from the RP cell to the AP cell. By considering the imaginary steady-state voltammogram at every interface of all the cells, we revealed that the membrane potential and the interfacial potentials of each cell are mutually changed by the generation of the circulating current due to the transfer of K^+ and Na^+. It became clear that the influence of the *iR* drop generated by the circulating current on the potential propagation was delayed and reduced, and that of the charging current was delayed. The authors propose that the hyperpolarization during the nerve conduction measured by the voltage-clamp method is caused by the inadequate evaluation on the relation between the membrane potential and the membrane current.

References

1 I. B. Levitan and L. K. Kaczmarek, *The Neuron: Cell and Molecular Biology*, Oxford University Press, New York, 3rd edn., 2002.

2 R. Phillips, J. Kondev and J. Theriot, *Physical Biology of the Cell*, Garland Science, New York, 2nd edn., 2009.

3 W. Schwarz and J. Rettinger, *Foundations of Electrophysiology*, Shaker, Germany, 2000.

4 B. Hille, *Ion Channels of Excitable Membrane*, Sinauer Associates, Sundeland, USA, 3rd edn., 2001.

5 Fundamental Neuroscience, ed. L. R. Squire, D. Berg, F. E. Bloom, S. du Lac, A. Ghosh and N. C. Spitzer, Elsevier, Amsterdam, 4th edn., 2012.

6 G. J. Kress and S. Mennerrick, *Neurosci*., 2009, **158**, 211-222.

7 A. L. Hodgkin and A. F. Huxley, *J. Physiol*., 1952, **117**, 500-544.

8 N. Ueya, O. Shirai, Y. Kushida, S. Tsujimura and K. Kano, *J. Electroanal. Chem*., 2012, **673**, 8-12.

9 Y. Kushida, O. Shirai, Y. Kitazumi and K. Kano, *Bull. Chem. Soc. Jpn*., 2014, **87**, 110-112.

10 Y. Kushida, O. Shirai, Y. Kitazumi and K. Kano, *Electroanalysis*, 2014, **26**, 1858-1865.

11 Y. Kushida, O.Shirai, Y. Takano, Y. Kitazumi and K. Kano, *Anal. Sci*., 2015, **31**, 677-683.

12 Y. Yoshida, M. Matsui, O. Shirai, K. Maeda, S. Kihara, *Anal. Chim. Acta*, 1998, **373**, 213-225.

13 Z. Samec, *Pure Appl. Chem*., 2004, **76**, 2147-2180.

14 M. H. P. Kole, S. U. Ilschner, B. M. Kampa, S. R. Williams, P. C. Ruben and G. J. Stuart, *Nat. Neurosci*., 2008, **11**, 178-186.

15 T. Tomita, *J. Theor. Biol*., 1966, **12**, 216-227.

16 D. Debanne, E. Campanac, A. Bialowas, E. Carlier, G. Alcaraz, *Physiol. Rev.*, 2011, **91**, 555-602.

17 S. Cullheim, *Neurosci. Lett*., 1978, **8**, 17-20. S. G. Waxman, and M. V. L. Bennett, *Nature*, 1972, **238**, 217-219.

Figure Captions

Fig.1 Overview of (A) a typical nerve cell, (B) a model system constructed by five liquid membrane cells (AP, RP and Rec1-3 cell) and (C) the structure of each cell.

Fig.2 The changes in (A) the membrane potential and in (B) the electric current of each cell. Solid line: Rec1 cell, broken line: Rec2 cell, dashed line: Rec3 cell, gray solid line: AP cell.

Fig.3 Imaginary steady-state voltammograms at the W1|M and W2|M interfaces. (A) The voltammogram at the W1|M interface of the Rec1 cell, (B) that at the W2|M interface of the Rec1 cell, (C) that at the W1|M interface of the Ap cell and (D) that at the W2|M interface of the AP cell.

Fig.4 The changes in (A) the membrane potentials of the Rec1-3 cells with different resistors, (B) the currents flowed at the Rec1-3 cells with different resistors, (C) the membrane potentials of the Rec1-3 cells with different capacitors and (D) the electric currents flowed at the Rec1-3 cells with different capacitors.
(A) and (B) Solid line: 5 kΩ, broken line: 10 kΩ, dashed line: 20 kΩ, dash-dotted line: 51 kΩ.
(C) and (D) Solid line: 0 μF, broken line: 10 μF, dashed line: 50 μF, dash-dotted line: 100 μF.

Fig.5 Illustration on the relation between the magnitude of circulating current and the distance in axon.

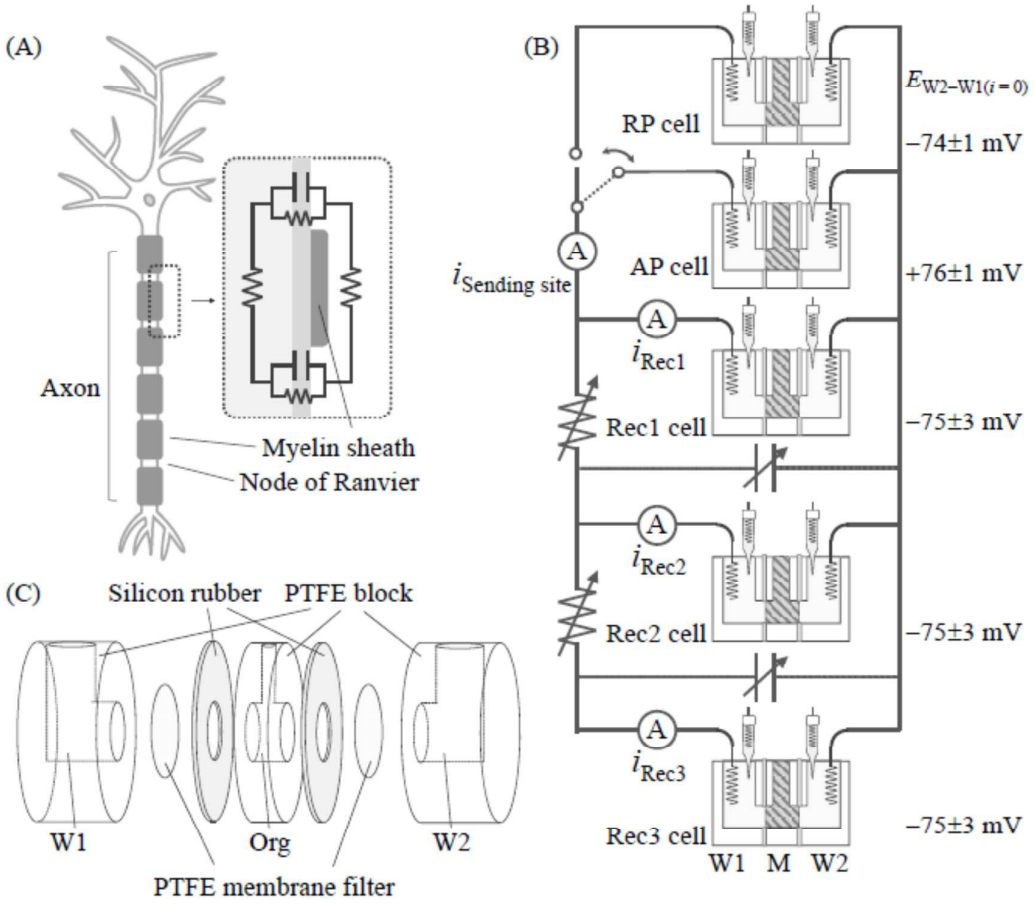

Fig.1 Y. Takano, et al.

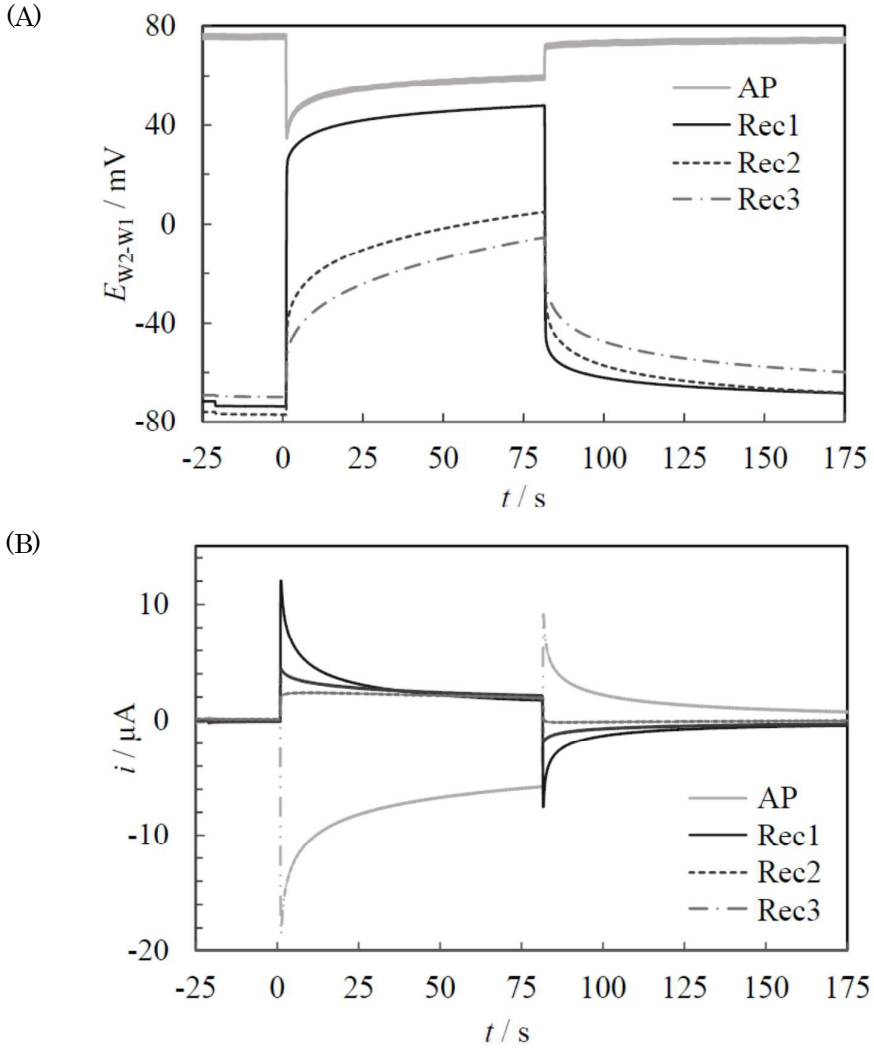

Fig.2 Y. Takano, et al.

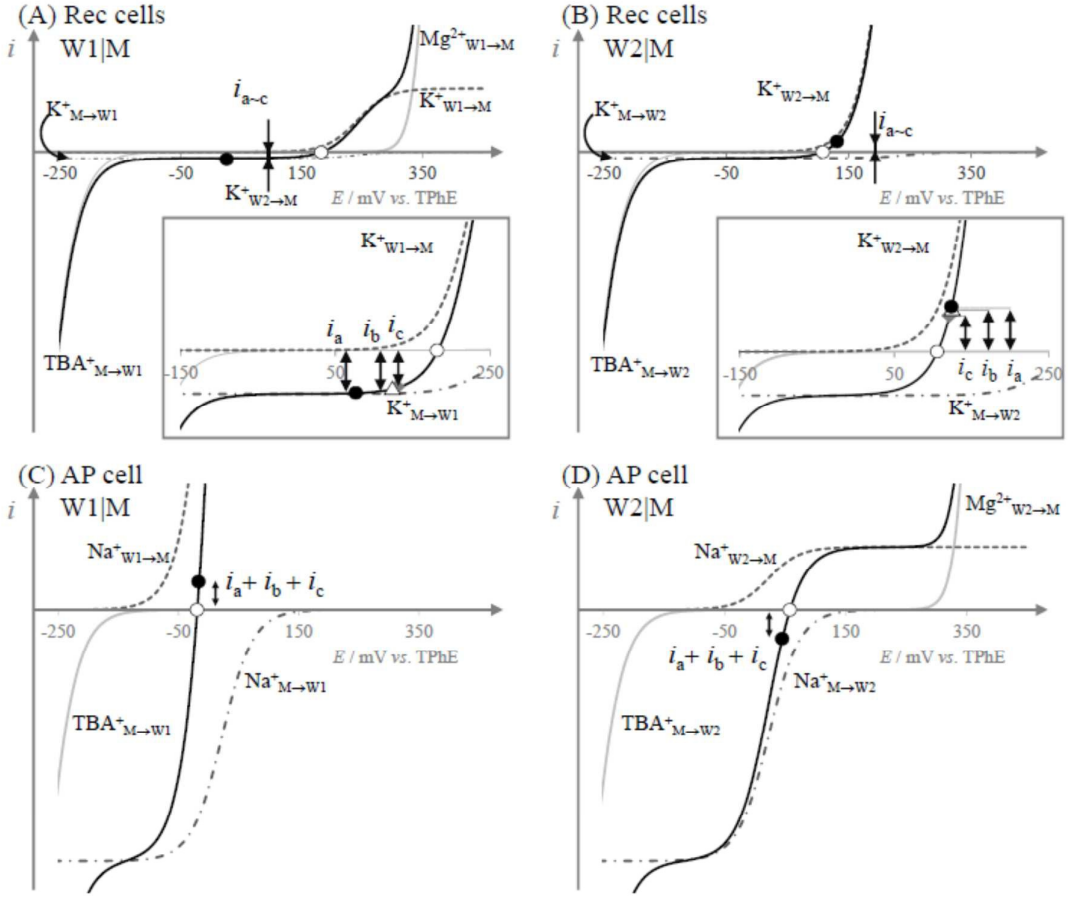

Fig.3 Y. Takano, et al.

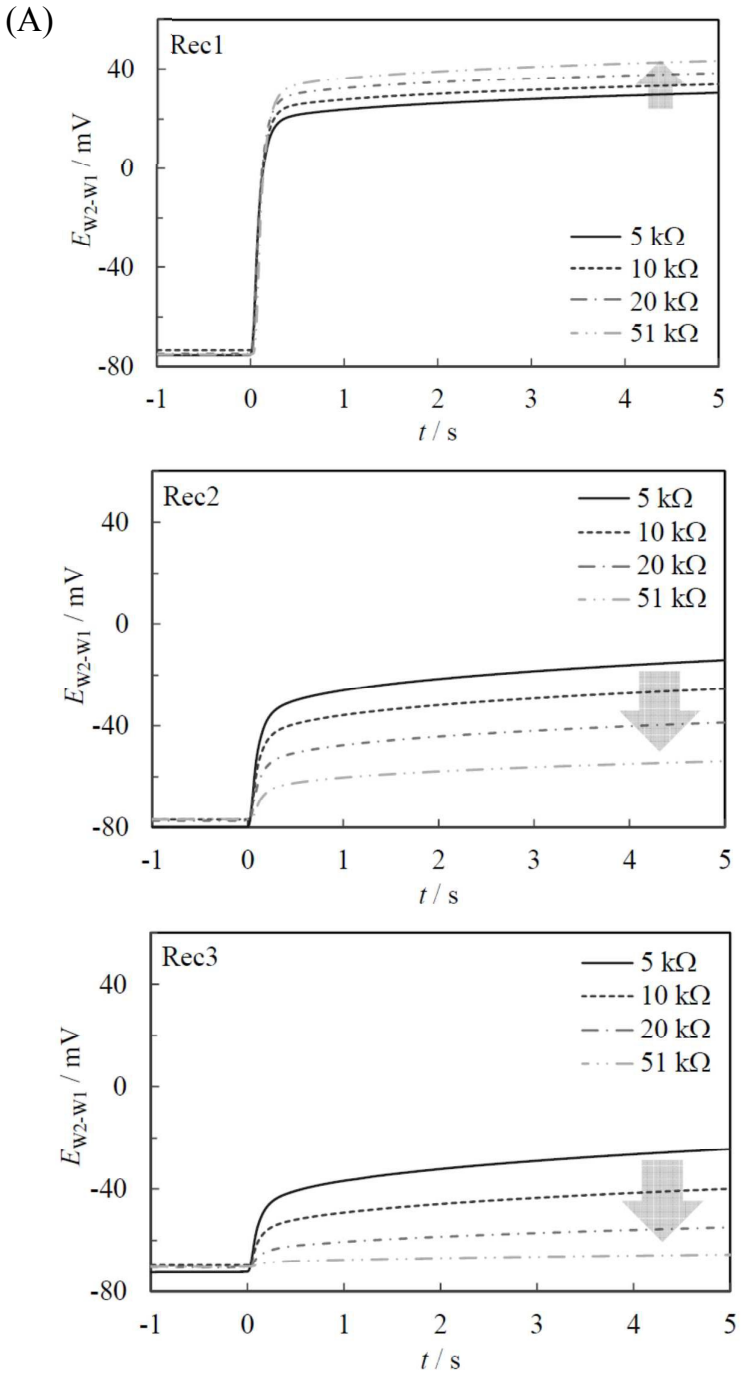

Fig.4(A) Y. Takano, et al.

(B)

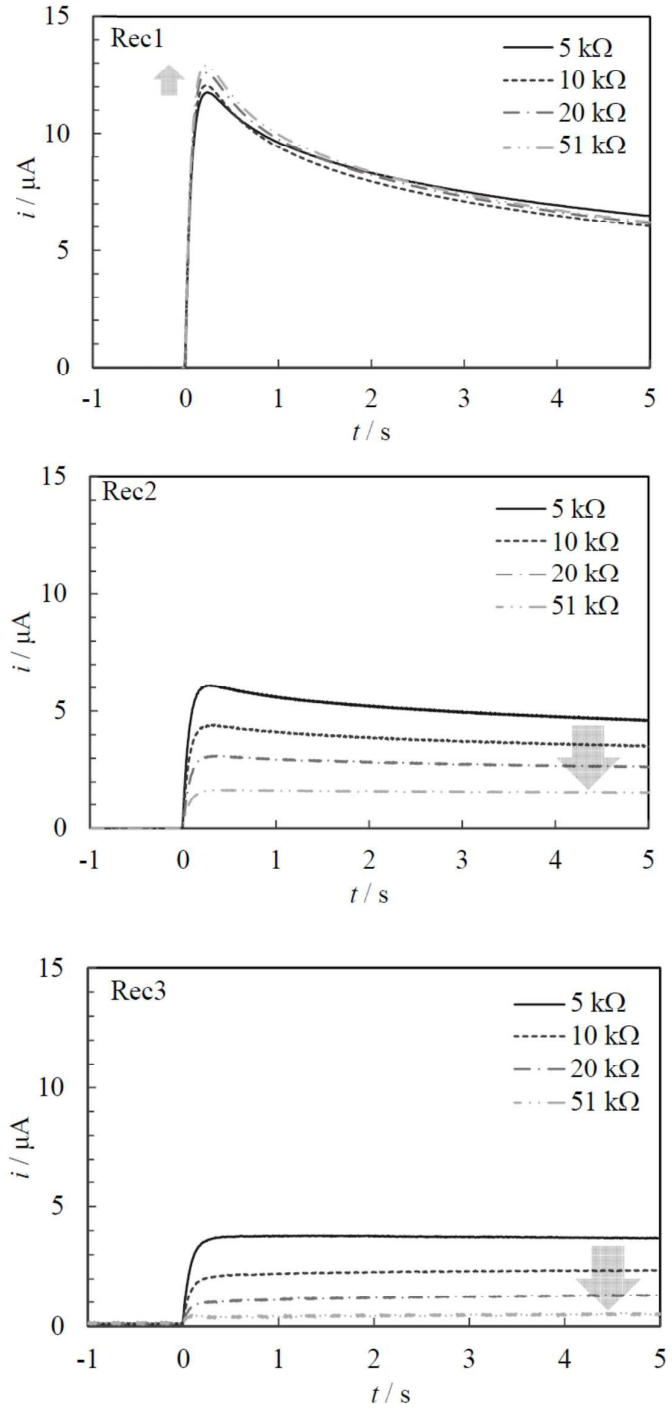

Fig.4(B) Y, Yakano, et al.

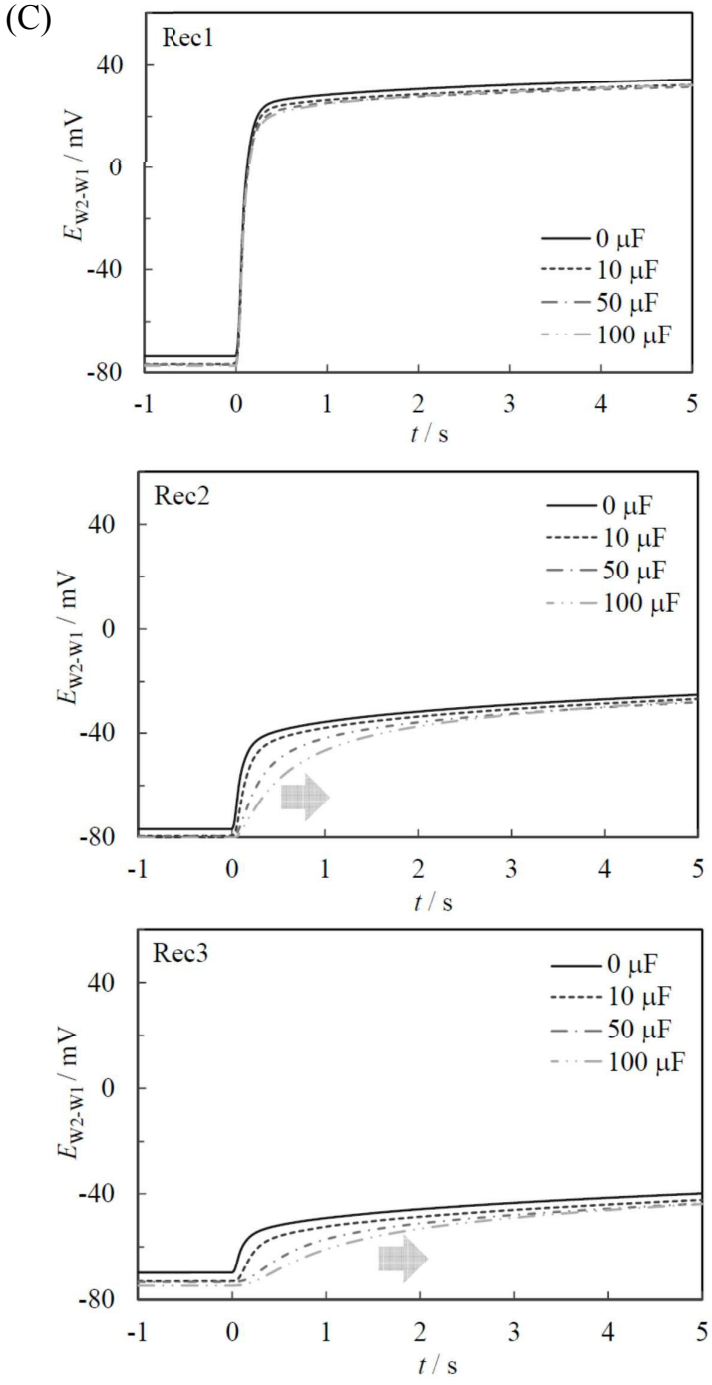

Fig.4(C) Y. Takano, et al.

(D)

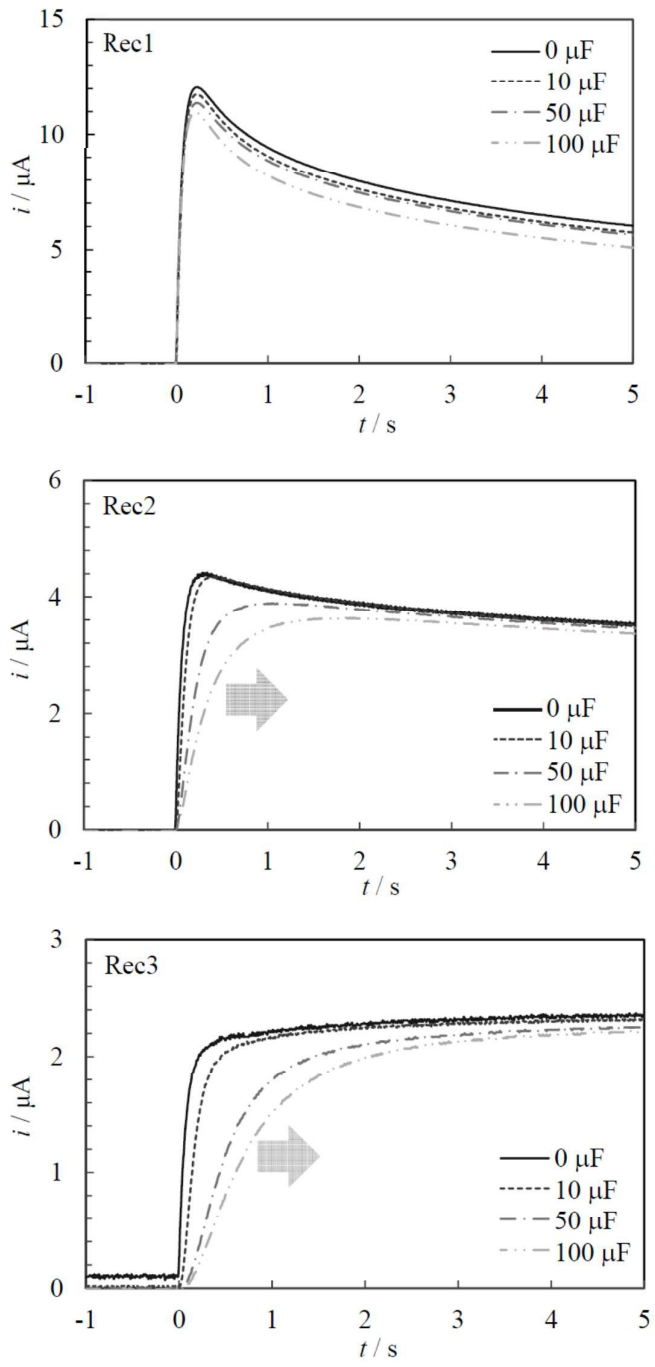

Fig.4(D) Y. Takano, et al.

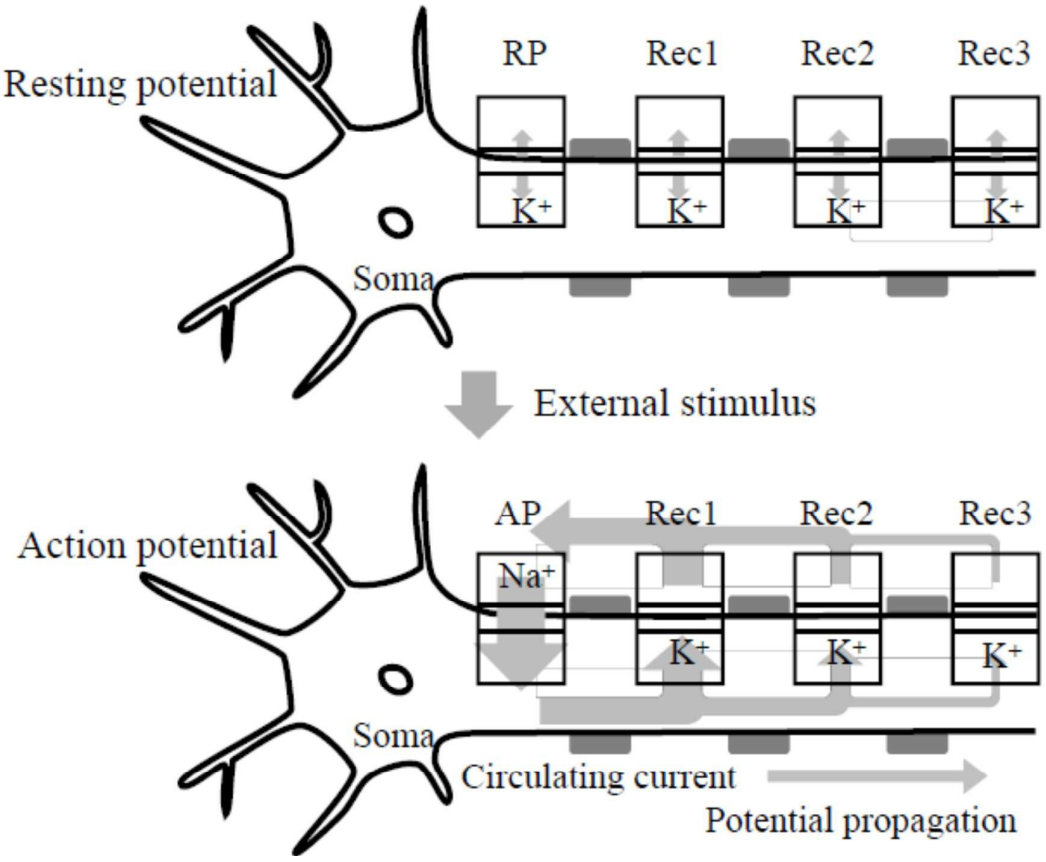

Fig.5 Y. Takano, et al.

Graphical abstract

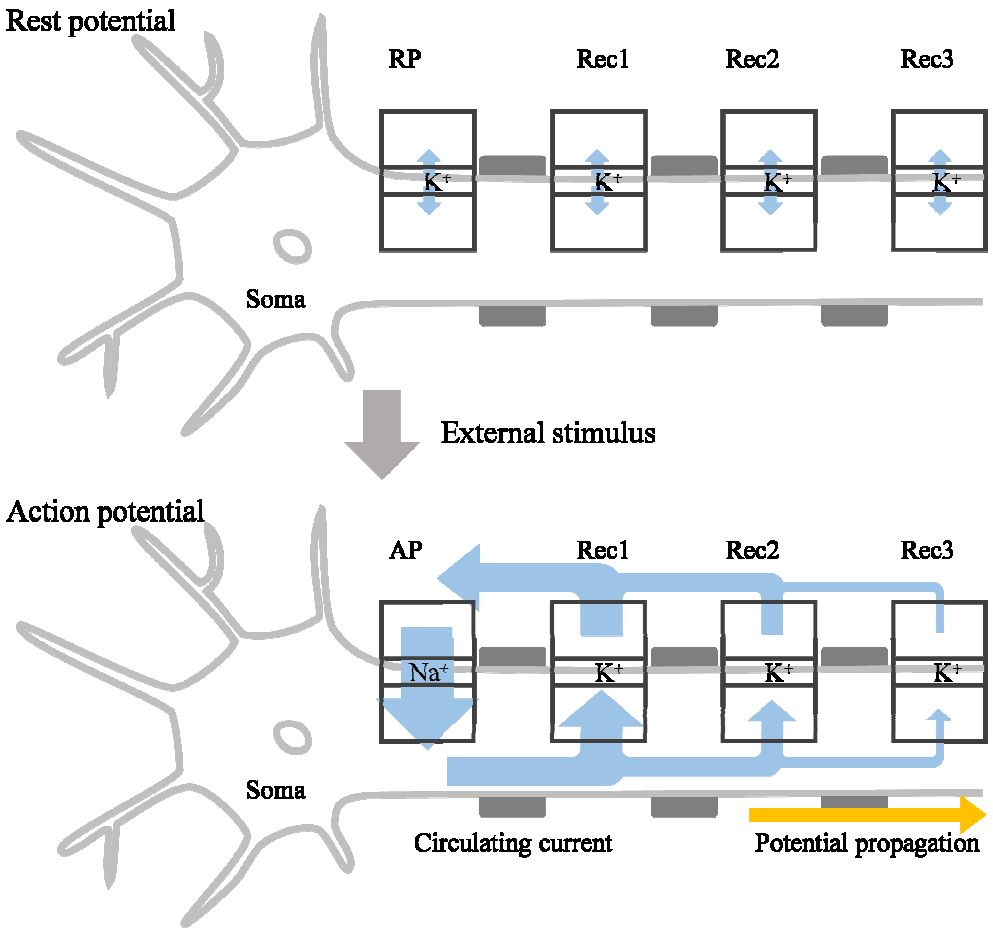

The relation between the magnitude of circulating current and the distance in axon.